



Original Article

Accumulated bladder wall dose is correlated with patient-reported acute urinary toxicity in prostate cancer patients treated with stereotactic, daily adaptive MR-guided radiotherapy



Thomas Willigenburg^{a,*}, Joanne M. van der Velden^a, Cornel Zachiu^a, Frederik R. Teunissen^a, Jan J.W. Lagendijk^a, Bas W. Raaymakers^a, Johannes C.J. de Boer^a, Jochem R.N. van der Voort van Zyp^a

^a University Medical Center Utrecht, Department of Radiation Oncology, The Netherlands

ARTICLE INFO

Article history:

Received 1 March 2022

Received in revised form 20 April 2022

Accepted 20 April 2022

Available online 28 April 2022

Keywords:

Bladder wall

Dose accumulation

MR-guided radiotherapy

Prostate cancer

SBRT

Urinary toxicity

ABSTRACT

Background and purpose: Magnetic resonance (MR)-guided linear accelerators (MR-Linac) enable accurate estimation of delivered doses through dose accumulation using daily MR images and treatment plans. We aimed to assess the association between the accumulated bladder (wall) dose and patient-reported acute urinary toxicity in prostate cancer (PCa) patients treated with stereotactic body radiation therapy (SBRT).

Materials and methods: One-hundred-and-thirty PCa patients treated on a 1.5 T MR-Linac were included. Patients filled out International Prostate Symptom Scores (IPSS) questionnaires at baseline, 1 month, and 3 months post-treatment. Deformable image registration-based dose accumulation was performed to reconstruct the delivered dose. Dose parameters for both bladder and bladder wall were correlated with a clinically relevant increase in IPSS (≥ 10 points) and/or start of alpha-blockers within 3 months using logistic regression.

Results: Thirty-nine patients (30%) experienced a clinically relevant IPSS increase and/or started with alpha-blockers. Bladder $D_{5\text{cm}^3}$, $V_{10-35\text{Gy}}$ (in %), and D_{mean} and Bladder wall $V_{10-35\text{Gy}}$ (cm^3 and %) and D_{mean} were correlated with the outcome (odds ratios 1.04–1.33, p -values 0.001–0.044). Corrected for baseline characteristics, bladder $V_{10-35\text{Gy}}$ (in %) and D_{mean} and bladder wall $V_{10-35\text{Gy}}$ (cm^3 and %) and D_{mean} were still correlated with the outcome (odds ratios 1.04–1.30, p -values 0.001–0.028). Bladder wall parameters generally showed larger AUC values.

Conclusion: This is the first study to assess the correlation between accumulated bladder wall dose and patient-reported urinary toxicity in PCa patients treated with MR-guided SBRT. The dose to the bladder wall is a promising parameter for prediction of patient-reported urinary toxicity and therefore warrants prospective validation and consideration in treatment planning.

© 2022 The Author(s). Published by Elsevier B.V. Radiotherapy and Oncology 171 (2022) 182–188 This is an open access article under the CC BY license (<http://creativecommons.org/licenses/by/4.0/>).

Stereotactic body radiation therapy (SBRT) has become a standard treatment for patients with low- and intermediate-risk prostate cancer (PCa). With this form of extreme hypofractionation, patients are commonly treated with 5 fractions of 7.25 Gy over the course of 1–2.5 weeks [1]. Oncological outcomes after SBRT are excellent, with 7-year biochemical failure-free survival rate of 93.7% [1].

Severe toxicity rates after prostate SBRT are low, with $\leq 1\%$ combined genitourinary (GU) and gastrointestinal (GI) grade ≥ 3 toxicity [1]. However, physician-reported incidences of acute grade

2 GU toxicity ranged between 21–28% in phase-3 trials comparing conventional treatment with SBRT [2,3]. Also, patient-reported outcome measures (PROMs), such as the International Prostate Symptom Score (IPSS) questionnaire, have shown clinically relevant side acute effects in a significant number of patients [3–7].

The introduction of magnetic resonance (MR)-guided linear accelerators (MR-Linac) has enabled intra-fraction MR imaging and daily plan adaptation [8,9]. While the potential clinical benefits of MR-guided treatment have yet to be established, the incorporation of high-quality MR imaging provides more detailed anatomical information shortly before and during the treatment compared to conventional systems [10–12]. With online plan adaptation, the treatment plan is adapted to fit the daily anatomy, thereby potentially increasing treatment effectiveness while also reducing radiation dose to organs-at-risk (OARs) [9]. Furthermore,

* Corresponding author at: University Medical Center Utrecht, Heidelberglaan 100, 3584 CX Utrecht, The Netherlands.

E-mail address: T.Willigenburg-3@umcutrecht.nl (T. Willigenburg).

¹ Postal address: Postbus 85500, 3508 GA Utrecht, Postal Room Q00.3.11, The Netherlands.

the daily repeated imaging and re-planning allow more accurate estimation of the actual delivered dose [13,14]. Additionally, the use of high-quality MR imaging enables identification of soft-tissue substructures, such as the bladder wall [15].

Currently, evidence on the relationship between the actual delivered dose to urinary structures and acute urinary toxicity after PCa SBRT is scarce as many studies considered pretreatment plan data only [16,17]. The aim of the current study was to gain insight into the dose–effect relationship between the accumulated bladder and bladder wall dose and patient-reported acute urinary toxicity in PCa patients treated with MR-guided SBRT.

Materials and methods

Patients and treatment procedures

For this study, PCa patients treated with 5 fractions of 7.25 Gy on a 1.5 T MR-Linac (Unity, Elekta AB, Stockholm, Sweden) between March 2020 and May 2021, who provided informed consent for the use of their data within the prospective Utrecht Prostate Cohort (UPC) study (NCT04228211), were identified. In the UPC study, patients with primary localized PCa are included before treatment and prospectively followed over time. After exclusion of 29 patients with missing baseline and/or follow-up IPSS data, 132 patients were included.

Patients were eligible for SBRT treatment in case of low- or intermediate-risk PCa (NCCN classification), IPSS ≤ 20, and good clinical condition (WHO performance status 0–2). No restrictions with respect to age and/or prostate size were applied. Seven patients with high-risk PCa, including two patients with cT3a PCa, were treated ‘off-protocol’ at the physician’s discretion (Table 1). Treatment was delivered in five fractions over the course of 2.5 weeks (two fractions per week). A dose of 36.25 Gy was prescribed to the planning target volume (PTV) (Supplementary Data A). The clinical target volume (CTV) included the prostate body, the gross tumor volume (GTV) with a 4 mm margin excluding OARs, and up to 1/3rd of the seminal vesicles. An isotropic CTV to

PTV margin of 5 mm was applied. All patients were treated with a so-called ‘Adapt-to-Shape’ workflow [9]. In short, during each fraction, an initial daily T2-weighted 3D MR scan (MR_{initial}) was acquired. Contours were propagated non-rigidly from the pre-treatment MR to the current daily MR scan. Next, the operator visually checked the propagated contours and – if needed – manually adapted them [18]. After contour approval, treatment plan optimization was initiated. Before the end of plan optimization, an additional MR scan was acquired for position verification (PV) purposes (MR_{PV}). In all patients, an additional virtual couch shift (VSC), also known as ‘Adapt-to-Position’ (ATP), was applied before treatment delivery in case of prostate shifts of > 1 mm between MR_{initial} and MR_{PV} (for details see [19]).

Dose accumulation and dosimetry parameters

The accumulated dose (Dose_{acc}) was reconstructed using the daily dose distributions (Dose_{fx1-5}) corresponding to the daily PV scans (MR_{PV1-5}), so that the latest anatomy prior to beam-on time was considered (Fig. 1). As previously reported, the time between MR_{PV} and beam-on in our cohort was on average 5 min compared to approximately 27 min between MR_{initial} and beam-on [19]. Therefore, dose calculation on MR_{PV} will ensure a better estimation of the actual delivered dose as compared to using MR_{initial} or the pre-treatment plan only. For image registration purposes and dose-volume analyses, the inner and outer bladder wall structures were delineated by two physicians on MR_{PV1-5} (Supplementary Data B). The bladder was defined as the entire volume circumscribed by the outer bladder wall, including the bladder content. The bladder wall was defined as the hollow structure bordered by the outer and inner bladder wall contours.

An in-house developed deformable image registration (DIR) algorithm and pipeline was used (‘Evolution’) [20], which was extended with dose accumulation possibilities [21]. The algorithm was chosen based on its previous successful employment for registering longitudinally-acquired MR images in PCa patients [21–23]. The delineated outer and inner bladder wall contours were used to

Table 1

Baseline patient, tumor, and treatment characteristics for the complete cohort and stratified by ‘IPSS + 10 and/or start of alpha-blockers within 3 months’: yes (Toxicity +) or no (Toxicity –).

		Total group	Toxicity +	Toxicity –
Number of patients (n)		130	39	91
Age in years (mean, SD)		69 (6)	68 (6)	69 (6)
Risk classification (NCCN) (n, %)	Low	14 (10.8)	5 (12.8)	9 (9.9)
	Intermediate	109 (83.8)	30 (76.9)	79 (86.8)
	High	7 (5.4)	4 (10.3)	3 (3.3)
Gleason score (n, %)	3 + 3 = 6	25 (19.2)	9 (23.1)	16 (17.6)
	3 + 4 = 7	79 (60.8)	24 (61.5)	55 (60.4)
	4 + 3 = 7	25 (19.2)	6 (15.4)	19 (20.9)
	8	1 (0.8)	0 (0)	1 (1.1)
cT-stage (n, %)	cT1	66 (50.8)	20 (51.3)	46 (50.5)
	cT2	62 (47.7)	19 (48.7)	43 (47.3)
	cT3	2 (1.5)	0 (0)	2 (2.2)
Diabetes Mellitus (n, %)	No	123 (94.6)	36 (92.3)	87 (95.6)
	Yes	7 (5.4)	3 (7.7)	4 (4.6)
Cardiovascular disease (n, %)	No	117 (90.0)	37 (94.9)	80 (87.9)
	Yes	13 (10.0)	2 (5.1)	11 (12.1)
Hormonal therapy (n, %)	No	122 (93.8)	36 (92.3)	86 (94.5)
	Yes	8 (6.2)	3 (7.7)	5 (5.5)
Alpha-blocker usage at baseline (n, %)	No	116 (89.2)	38 (97.4)	78 (85.7)
	Yes	14 (10.8)	1 (2.6)	13 (14.3)
PTV in cm ³ (median, IQR)		100 (84–122)	114 (102–134)	93 (80–114)
Mean* bladder volume in cm ³ (median, IQR)		153 (115–207)	137 (113–190)	162 (118–225)
Mean* bladder wall volume in cm ³ (median, IQR)		41 (34–47)	40 (33–47)	41 (36–47)
Baseline IPSS (median, IQR)		6 (4–10)	7 (4–9)	6 (3–11)

Legend: SD = standard deviation. NCCN = National Comprehensive Cancer Network. IQR = interquartile range. IPSS = international prostate symptom score. *Mean bladder (wall) volume over the five-course treatment.

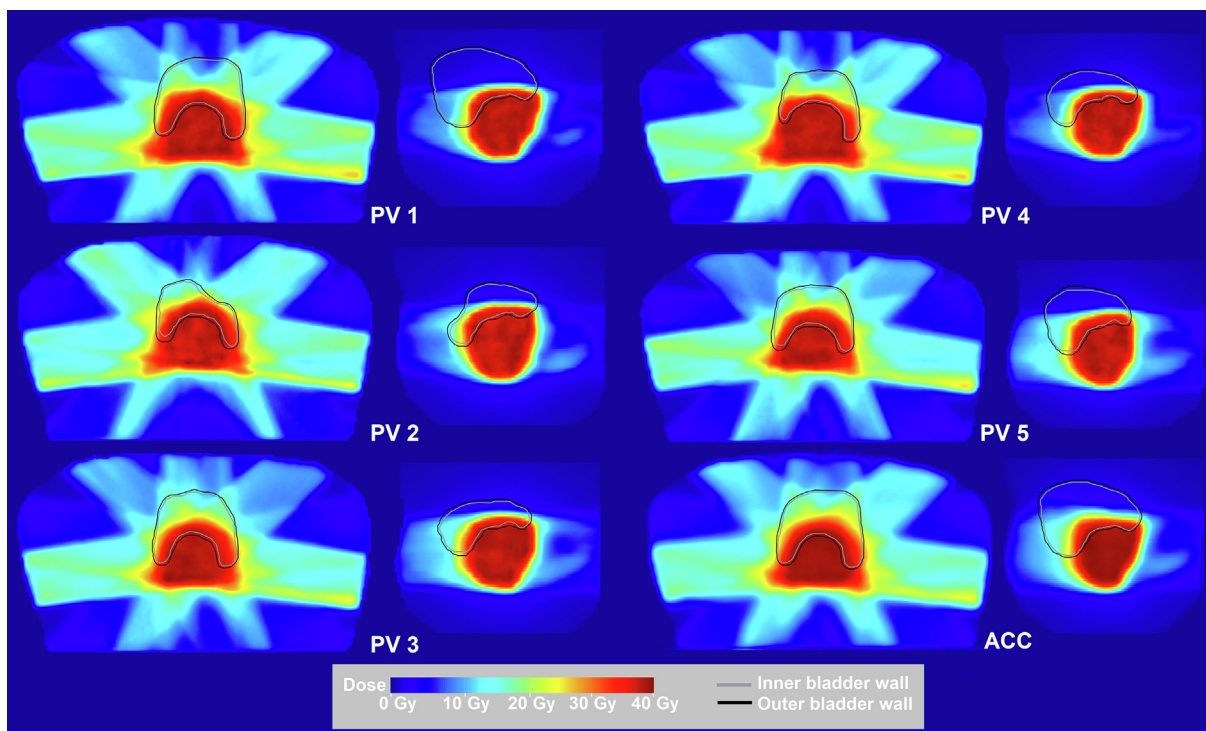


Fig. 1. Exemplary dose distributions (left: transversal slice; right: sagittal slice) for the anatomy on the position verification (PV) scan of fraction 1–5 and the accumulated dose distribution (ACC) on the reference anatomy (PV 1 for this case). The outer and inner bladder wall contours are displayed in black and grey.

guide the registration process. $Dose_{fx1-5}$ for each scan (MR_{PV1-5}) was calculated based on the corresponding treatment plan (Fig. 1). Next, MR_{PV2-5} were registered to MR_{PV1} (reference), resulting in four deformation vector fields (DVF) for each patient. The DVF were used to map the dose distribution to the reference image using the energy-per-mass transfer technique [21]. Dice similarity coefficient (DSC) and Hausdorff distance (HD) were calculated for the bladder and bladder wall structures (delineated versus propagated) to evaluate the DVF of MR_{PV2-5} to MR_{PV1} . For each case, the mean DSC and HD (DSC_{mean} and HD_{mean}) over the four registrations were calculated. Outliers were identified based on DSC and HD and visually checked to assess the location and extent of misregistration. In case of registration errors due to large bladder volume differences between MR_{PV1} and MR_{PV2-5} , a different reference scan was used. Granted the results were satisfying, the case was included for dose-toxicity analyses. Two cases were excluded from dose-toxicity analyses due to misregistrations near the prostate-bladder interface, which could not be resolved by using a different reference scan.

The following bladder (wall) dose parameters were extracted from $Dose_{acc}$: absolute (cm^3) and relative (%) volume receiving 10–35 Gy ($V_{10-35Gy}$) in 5 Gy bins and 37 Gy (V_{37Gy}), mean dose (D_{mean}) in Gy, and dose (Gy) to the 1 and 5 cm^3 receiving the highest dose ($D1cm^3$ and $D5cm^3$).

Urinary toxicity and patient-reported outcome measurements

In the UPC study, toxicity was prospectively registered using both physician-reported outcome measurements and PROMs at baseline and during follow-up, including at one (1M) and three months (3M) post-treatment. Patients filled out several general and domain-specific health-related quality-of-life questionnaires. For this study, we focused on the IPSS. The primary outcome, acute urinary toxicity, was defined as an IPSS increase of ≥ 10 points (IPSS + 10) from baseline on more than one occasion within three

months after treatment, as frequently used in other studies [16,24]. Since patients sometimes start with alpha-blocking medication (e.g., tamsulosin) shortly after treatment in case of significant urinary complaints, this might mask an increase in IPSS. Therefore, we assessed a combined outcome: an increase in IPSS of ≥ 10 points from baseline and/or start of alpha-blocking medication within 3 months post-treatment.

Statistical analysis

Descriptive statistics were reported for baseline patient-, tumor-, and treatment characteristics. Categorical variables were summarized using absolute numbers and percentages. For continuous variables mean and standard deviation or median and interquartile range (IQR) were used, for normally distributed and skewed data, respectively. Significant differences in baseline characteristics between those with and without toxicity were reported. Differences in IPSS between baseline and 1M and 3M were assessed using the Wilcoxon signed rank test. p -values < 0.05 were considered statistically significant.

To show the crude effect, correlations between dosimetry parameters and the combined outcome were assessed using univariable logistic regression analysis. Additionally, area under the receiver-operating-characteristic (ROC) curve (AUC) was calculated for each dose parameter and Pearson's correlation coefficients were calculated between dose parameters. Multivariable logistic regression analysis was performed, providing odds ratios (OR) corrected for the following available baseline characteristics: age (continuous), diabetes, cardiovascular disease, baseline IPSS (continuous), and alpha-blocker usage at baseline.

Dose-effect curves were plotted for a selection of dose parameters that showed the highest correlation with the outcome (bladder D_{mean} and bladder wall D_{mean} and V_{25Gy} in cm^3) using the corrected OR. Finally, preliminary dose cut-off values for these dose parameters were determined using the ROC-curve, with the

optimal constraint – that best discriminates between those with and without the outcome – determined by the Youden index [25].

All statistical analyses were performed using SPSS version 26 (IBM® SPSS Statistics, Armonk, New York, United States of America) and R Studio (version 4.1.2, R Foundation for Statistical Computing, Vienna, Austria, <https://rstudio.com>).

Results

One-hundred-and-thirty patients were included, of whom 39 patients (30%) experienced acute urinary toxicity (Table 1). Of these 39 patients, 20 patients reported an increase in IPSS of ≥ 10 points during the first three months of follow-up, of whom 10 also started with alpha-blocking medication. The remaining 19 patients reported no increase in IPSS of > 10 points but did start with alpha-blocking medication. Patients with and without acute urinary toxicity were comparable at baseline except for PTV volume ($p < 0.001$) and alpha-blocker usage at baseline ($p = 0.048$). Median IPSS for the entire cohort was significantly higher at 1M ($p < 0.001$) and 3M ($p = 0.001$) compared to baseline, with a larger proportion of patients experiencing moderate (59.5%) or severe (11.9%) urinary symptoms at 1M (Fig. 2). Most patients reported an increase in score for the ‘frequency’, ‘urgency’, and ‘weak stream’ sub-items (results not presented).

Median (IQR) DSC_{mean} was 0.99 (0.98–0.99) for the bladder and 0.84 (0.80–0.87) for the bladder wall. Median (IQR) HD_{mean} was 0.05 mm (0.03–0.10) for the bladder and 0.57 mm (0.42–0.83) for the bladder wall. For two cases (1.5%), bladder DSC_{mean} was < 0.95 (0.92 and 0.94), due to large bladder volume differences that caused (small) registration errors in the cranial part of the bladder

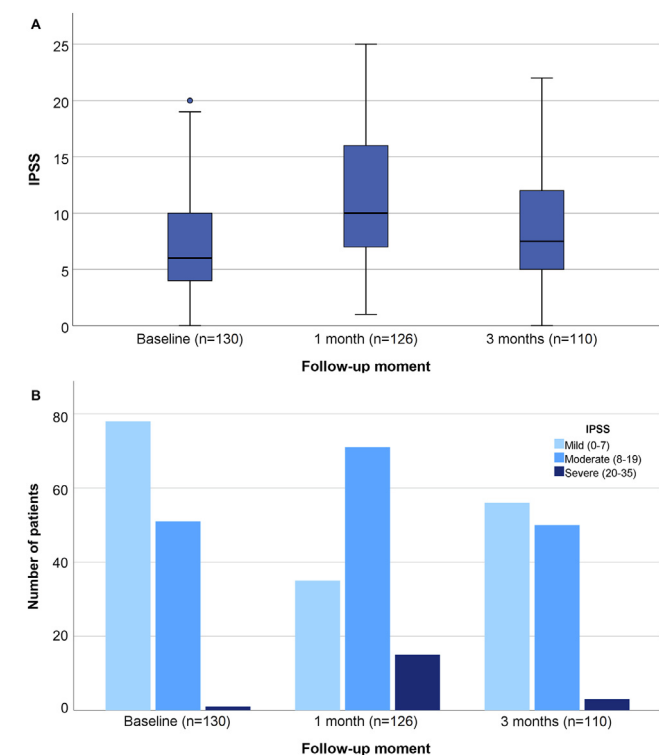


Fig. 2. (A) Boxplots of IPSS at baseline, 1 month, and 3 months post-treatment. Black horizontal bars indicate the median, the boxes indicate the 25–75th percentiles. Error bars indicate the 95% confidence intervals. Outliers (< 25 th percentile – $1.5 \times$ interquartile range or > 75 th percentile + $1.5 \times$ interquartile range) are indicated as separate dots. (B) Distribution of IPSS severity groups (mild, moderate, severe) at baseline, 1 month, and 3 months post-treatment.

Table 2

Univariable logistic regression analysis (odds ratios [OR]) with 95% confidence intervals (CI) and area under the receiver-operating-characteristic curve (AUC) for IPSS + 10 and/or start of alpha-blockers within 3 months post-treatment. Findings with a p -value < 0.05 are indicated in bold.

	Odds ratio	95% CI OR	p -value	AUC	95% CI AUC
Bladder					
V _{10Gy} (cm ³)	1.01	0.99–1.02	0.29	0.59	0.49–0.70
V _{15Gy} (cm ³)	1.01	0.99–1.03	0.28	0.58	0.48–0.69
V _{20Gy} (cm ³)	1.01	0.99–1.04	0.29	0.59	0.49–0.69
V _{25Gy} (cm ³)	1.02	0.98–1.05	0.29	0.59	0.49–0.69
V _{30Gy} (cm ³)	1.03	0.98–1.08	0.28	0.60	0.50–0.70
V _{35Gy} (cm ³)	1.05	0.96–1.16	0.27	0.60	0.50–0.70
V _{37Gy} (cm ³)	1.05	0.89–1.23	0.55	0.57	0.47–0.68
V _{10Gy} (%)	1.04	1.02–1.07	0.002	0.67	0.58–0.77
V _{15Gy} (%)	1.05	1.01–1.08	0.004	0.66	0.57–0.76
V _{20Gy} (%)	1.06	1.02–1.10	0.007	0.66	0.56–0.75
V _{25Gy} (%)	1.08	1.02–1.13	0.008	0.66	0.56–0.75
V _{30Gy} (%)	1.11	1.02–1.12	0.011	0.66	0.56–0.75
V _{35Gy} (%)	1.18	1.02–1.37	0.024	0.66	0.56–0.75
V _{37Gy} (%)	1.13	0.88–1.45	0.33	0.59	0.49–0.69
D _{mean}	1.19	1.07–1.33	0.002	0.67	0.58–0.76
D1cm ³	1.68	0.91–3.09	0.095	0.58	0.48–0.68
D5cm ³	1.33	1.01–1.74	0.044	0.61	0.51–0.71
Bladder wall					
V _{10Gy} (cm ³)	1.10	1.03–1.18	0.006	0.65	0.54–0.75
V _{15Gy} (cm ³)	1.13	1.04–1.24	0.006	0.64	0.54–0.75
V _{20Gy} (cm ³)	1.16	1.04–1.30	0.007	0.64	0.54–0.75
V _{25Gy} (cm ³)	1.20	1.05–1.37	0.006	0.65	0.55–0.76
V _{30Gy} (cm ³)	1.24	1.06–1.46	0.007	0.65	0.55–0.75
V _{35Gy} (cm ³)	1.29	1.05–1.59	0.016	0.64	0.54–0.74
V _{37Gy} (cm ³)	1.45	0.90–1.45	0.26	0.58	0.48–0.68
V _{10Gy} (%)	1.06	1.02–1.10	0.002	0.69	0.60–0.78
V _{15Gy} (%)	1.07	1.02–1.13	0.003	0.67	0.58–0.77
V _{20Gy} (%)	1.09	1.03–1.16	0.003	0.68	0.58–0.77
V _{25Gy} (%)	1.11	1.04–1.19	0.003	0.68	0.58–0.77
V _{30Gy} (%)	1.12	1.04–1.21	0.004	0.67	0.57–0.76
V _{35Gy} (%)	1.12	1.02–1.22	0.016	0.65	0.55–0.75
V _{37Gy} (%)	1.06	0.96–1.16	0.26	0.58	0.48–0.68
D _{mean}	1.28	1.10–1.48	0.001	0.69	0.60–0.78
D1cm ³	1.75	0.95–3.21	0.071	0.59	0.49–0.70
D5cm ³	1.11	1.00–1.24	0.058	0.62	0.52–0.73

for ≥ 1 registration. Because this was outside the medium–high dose area, these cases were included.

Collinearity statistics showed high correlations over the entire range of bladder (wall) dose parameters (Supplementary Data C). In univariable analysis (Table 2), Bladder D5cm³, V_{10–35Gy} (in %), and D_{mean} and Bladder wall V_{10–35Gy} (cm³ and %) and D_{mean} were correlated with the outcome (odds ratios 1.04–1.33, p -values 0.001–0.044). Except for relative V_{35–37Gy} (%), bladder wall dose parameters showed larger AUC values compared to their bladder equivalent (Table 2). Corrected for age, diabetes, cardiovascular disease, baseline IPSS, and alpha-blocker usage at baseline (Table 3), bladder V_{10–35Gy} (in %) and D_{mean} and bladder wall V_{10–35Gy} (cm³ and %) and D_{mean} were still correlated with the outcome (odds ratios 1.04–1.30, p -values 0.001–0.028).

Preliminary cut-off points for the dose parameters based on the Youden index were 11.2 Gy and 11.7 Gy for the bladder and bladder wall D_{mean}, respectively, and 9.0 cm³ for bladder wall V_{25Gy} (Fig. 3 and Supplementary Data D). In our cohort, of all patients with bladder wall V_{25Gy} ≤ 9.0 cm³ ($n = 70$), 16.6% reported urinary toxicity. For bladder wall D_{mean} ≤ 11.7 Gy ($n = 47$) this was 10.6%.

Discussion

Our study suggests a strong relationship between D_{mean} as well as low-medium doses (V_{10–35Gy}) to the bladder and bladder wall and patient-reported acute urinary toxicity in PCa patients treated

Table 3

Corrected* odds ratios (OR) in multivariable logistic regression analysis for IPSS + 10 and/or start of alpha-blockers within 3 months post-treatment. Findings with a *p*-value < 0.05 are indicated in bold.

	Corrected OR*	95% CI	<i>p</i> -value
<i>Bladder</i>			
V _{10Gy} (cm ³)	1.01	0.99–1.02	0.46
V _{15Gy} (cm ³)	1.01	0.99–1.03	0.43
V _{20Gy} (cm ³)	1.01	0.98–1.04	0.43
V _{25Gy} (cm ³)	1.02	0.98–1.06	0.42
V _{30Gy} (cm ³)	1.02	0.97–1.08	0.41
V _{35Gy} (cm ³)	1.05	0.95–1.16	0.36
V _{37Gy} (cm ³)	1.05	0.89–1.25	0.57
V _{10Gy} (%)	1.04	1.02–1.07	0.002
V _{15Gy} (%)	1.05	1.02–1.08	0.004
V _{20Gy} (%)	1.06	1.02–1.11	0.007
V _{25Gy} (%)	1.08	1.02–1.15	0.009
V _{30Gy} (%)	1.12	1.02–1.21	0.012
V _{35Gy} (%)	1.19	1.02–1.39	0.025
V _{37Gy} (%)	1.14	0.88–1.47	0.33
D _{mean}	1.20	1.07–1.35	0.002
D1cm ³	1.67	0.87–3.20	0.12
D5cm ³	1.34	0.99–1.81	0.06
<i>Bladder wall</i>			
V _{10Gy} (cm ³)	1.11	1.03–1.20	0.008
V _{15Gy} (cm ³)	1.14	1.03–1.25	0.011
V _{20Gy} (cm ³)	1.17	1.03–1.32	0.013
V _{25Gy} (cm ³)	1.21	1.04–1.41	0.013
V _{30Gy} (cm ³)	1.25	1.04–1.50	0.015
V _{35Gy} (cm ³)	1.30	1.03–1.64	0.027
V _{37Gy} (cm ³)	1.15	0.89–1.47	0.29
V _{10Gy} (%)	1.06	1.02–1.10	0.003
V _{15Gy} (%)	1.08	1.02–1.13	0.004
V _{20Gy} (%)	1.09	1.03–1.16	0.005
V _{25Gy} (%)	1.11	1.03–1.19	0.005
V _{30Gy} (%)	1.12	1.03–1.22	0.008
V _{35Gy} (%)	1.11	1.01–1.22	0.028
V _{37Gy} (%)	1.05	0.95–1.16	0.31
D _{mean}	1.29	1.10–1.51	0.001
D1cm ³	1.72	0.90–3.31	0.10
D5cm ³	1.10	0.98–1.25	0.11

*Corrected for: age (years), diabetes (yes/no), cardiovascular disease (yes/no), baseline IPSS, and alpha-blocker usage at baseline (yes/no).

with MR-guided SBRT. These correlations persisted after correction for multiple baseline characteristics. This is the first study to identify such a relationship for the bladder wall using the accumulated dose over the five treatment fractions. Based on our results, we suggest the use of constraints for bladder wall V_{25Gy} (cm³) and bladder (wall) D_{mean} for treatment planning for MR-guided PCa SBRT. Prospective validation of the suggested (soft) constraints is warranted. Furthermore, future research should focus on determination of the optimal constraints, feasibility of these constraints in treatment planning, and finally the clinical effects with respect to acute urinary toxicity.

While some of the bladder dose parameters were associated with the outcome, these associations seemed generally weaker (lower AUC values) compared to those for the bladder wall. This suggests higher accuracy of the bladder wall dose in predicting toxicity and is in line with the hypothesis that irradiation of the bladder wall – and not bladder content – induces toxicity. For the relative dose parameters (V_{10–37Gy} in % and D_{mean}), correlations between the bladder and bladder wall were high, whereas for absolute V_{10–30Gy} (cm³), correlations between the bladder and bladder wall dose were generally weaker except for the highest dose-volumes (Supplementary Data C). This probably is caused by the fact that the lower absolute bladder dose volumes also include large parts of bladder content. Together with the lack of

significant correlations for the absolute bladder dose parameters, this suggests that the absolute bladder volume receiving X Gy is not a sufficient proxy for the bladder wall. Although the bladder wall parameters showed higher predictive value (based on AUC), the relative bladder dose parameters might be a sufficient proxy, especially for D_{mean}. Absolute volumetric constraints are more practical because they do not require (online) delineation of the entire organ. However, concerning absolute dose parameters, we only found significant correlations for the bladder wall, and therefore we suggest delineating the bladder wall to be able to use for example V_{25Gy} (cm³) in treatment planning. Especially for the bladder wall, absolute volumetric constraints can be used, since bladder wall volume does not change over the course of treatment.

Since D_{mean} seems important in the prediction of acute urinary toxicity, the bladder size during treatment could contribute to the risk of toxicity. Mean bladder volume was larger (but not statistically significant) in the non-toxicity group compared to the group of patients with toxicity (Table 1). No strict bladder filling protocol was applied and therefore bladder size varied significantly between fractions and patients. A bladder filling protocol aimed at a stable, (comfortably) filled bladder could potentially reduce the mean dose and thereby reduce the risk of toxicity [26]. In addition, improvements in delivery accuracy, i.e., smaller PTV margins, are warranted to significantly reduce the dose to the entire bladder (wall) while providing adequate target coverage. To achieve this, fast, online-adaptive techniques are needed to counteract intra-fraction motion [27,28].

Acute patient-reported urinary toxicity was observed in 30% of our cohort in the first three months following treatment. While these numbers seem a bit high compared to other reports, we used a different definition of ‘patient-reported acute urinary toxicity’ compared to IPSS + 10 only [16,29,30]. In our study, only 15.4% (20/130) reported an increase in IPSS of ≥ 10 points. However, many patients started with alpha-blocking medication during or shortly after treatment, in case of (severe) irritative urinary complaints. Our pre-defined hypothesis was that the use of alpha-blocking medication might therefore mask an increase in IPSS during follow-up and thus dilute the correlation if not considered. As a sensitivity analysis (data not shown), we performed univariable logistic regression analysis for IPSS + 10 as the only outcome. Although the trends of the OR were consistent with the presented results, this yielded no significant correlations. This may partly be attributed to a lack of power with only 20 cases. Nevertheless, significant correlations between dosimetry and IPSS + 10 have been reported previously [16,24]. This discrepancy might be caused by using different assessment time-points during follow-up; Bohoudi et al. measured IPSS also at the end of treatment and Henderson et al. measured IPSS two weeks after the end of treatment compared to our first measurement at 1M post-treatment [16,24]. This leads to a difference in the sensitivity, as it is likely that a larger proportion will report significant urinary toxicity shortly after treatment. This is also reflected in the differences in incidence of IPSS + 10. Furthermore, differences in prescription of alpha-blocking medication could also attribute to this effect. Additionally, a sensitivity analysis was performed in those without alpha-blocking medication at baseline (*n* = 116, data not shown). This did not alter the results (OR) in a meaningful way, besides resulting in slightly higher *p*-values due to a smaller sample size.

To our knowledge, only Bohoudi et al. investigated the relationship between the accumulated dose to the bladder and urinary toxicity in PCa patients treated with adaptive MR-guided SBRT on a 0.35 T MR-Linac [16]. Considering only the dose to the entire bladder, similar medium-high accumulated dose levels (V_{20–32Gy} in

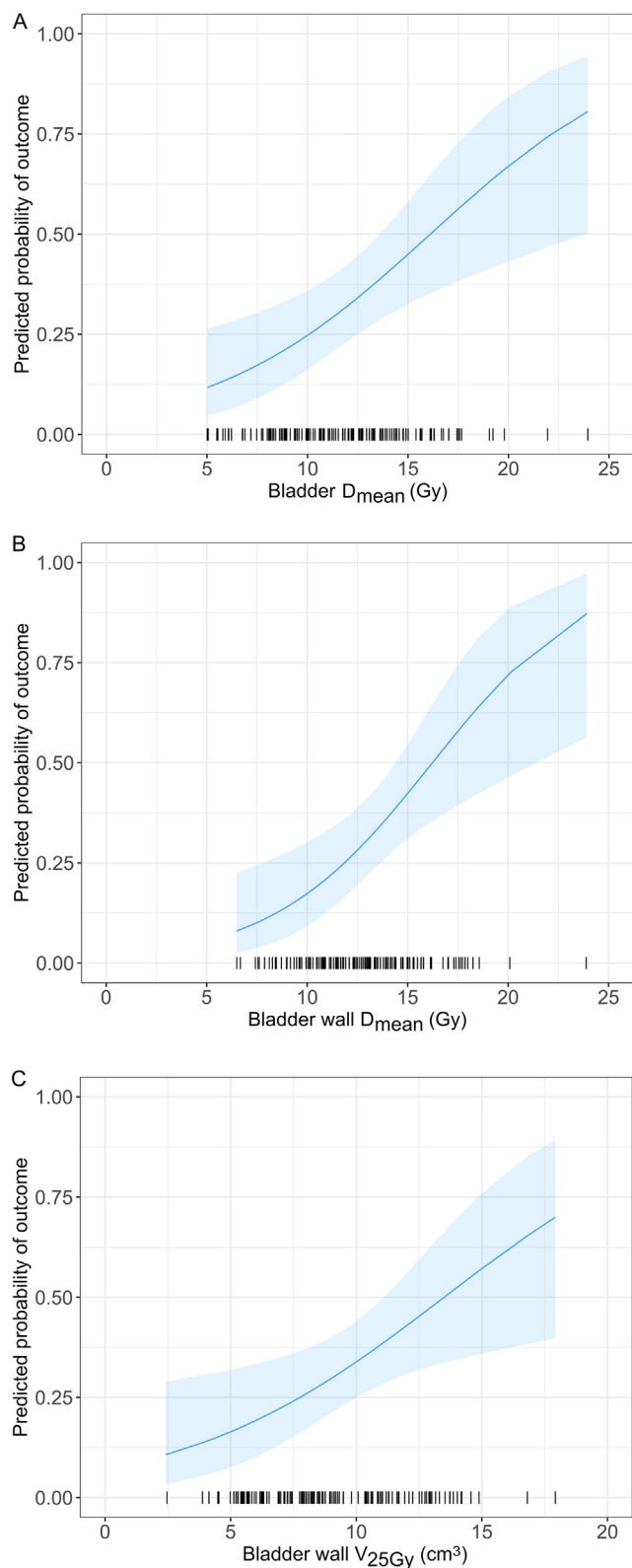


Fig. 3. Predicted probabilities of IPSS + 10 and/or start of alpha-blocking medication within 3 months post-treatment at various levels of bladder D_{mean} (A), bladder wall D_{mean} (B), and bladder wall V_{25Gy} in cm^3 (C), based on the corrected odds ratio. Modelled marginal means and their 95% confidence intervals are shown. The black vertical bars represent the values of the dose parameters for the individual patients in the cohort.

cm^3) were correlated with IPSS + 10. No correlations were found for the pretreatment plan. No relative dose parameters were assessed. Our results do not confirm the significant correlations found for absolute bladder dose parameters. This might have several explanations, besides the difference in primary outcome definition. First, as previously mentioned, the outcome was measured at different follow-up moments, leading to differences in toxicity rates. This could lead to differences in the sensitivity of the analyses that were performed. Finally, no multivariable analysis was performed, and therefore it is unclear if the observed correlations would persist when corrected for other (potentially) important clinical variables. Still, this study clearly indicates that the pretreatment dose cannot necessarily be used as a substitute for the actual delivered dose. Therefore, the accumulated dose should be considered.

Our study has some limitations. First, the exploratory aspects of the study should be interpreted with caution since no independent validation has yet been performed. For the bladder wall, however, the results were significant for almost the entire range of dose parameters, even after correction for baseline characteristics that are potentially related to the outcome, thus strongly suggesting the important role of bladder wall dose in the development of acute urinary toxicity. Although we did correct for several baseline characteristics, we cannot conclude that the found correlations are entirely causal, since residual confounding due to other to unmeasured and/or unknown variables could be present.

Second, manual delineation of the bladder wall is labor-intensive. This makes it less practical for an online workflow, in which contours are generated while the patient is on the treatment couch. Improved automatic segmentation could make use of the bladder wall in clinical online planning feasible. Furthermore, the use of bladder surface histograms might be an easier alternative to delineating the entire bladder wall. However, this does not take into account bladder wall thickness differences within the bladder and variation in thickness with bladder filling status, which impacts its accuracy [31,32].

Third, the inter-fraction dose accumulation pipeline we applied does not consider intra-fraction motion that occurs between MR_{PV} acquisition and end of beam-on. We have previously shown that significant intra-fraction motion can occur, and this might affect the delivered dose [10,13]. Intra-fraction dose accumulation, in addition to inter-fraction dose accumulation, will probably yield an even better approximation of the actual dose compared to inter-fraction dose accumulation only. Nevertheless, we tried to minimize the effect of intra-fraction motion in the current study by using the MR_{PV} that is acquired shortly before beam-on time.

Concluding, we have shown that the accumulated dose to the bladder (wall) is highly correlated with patient-reported acute urinary toxicity in PCa patients treated with daily adaptive MR-guided SBRT. These correlations persisted after correction for several baseline characteristics. Our results suggests that bladder wall dosimetry is preferred over whole bladder dosimetry in case one wishes to predict acute urinary toxicity as accurately as possible, although further research should validate these findings. The preliminary dose constraints could be used as a starting point for defining stricter dose constraints for prostate SBRT, with the aim of reducing clinically relevant acute urinary toxicity in these patients.

Funding

This research has been partly funded by ZonMw IMDI/LSH-TKI Foundation (The Netherlands, project number 104006004). The

funding sources were not involved in the design of the study, the collection, analysis, and interpretation of the data, nor in the writing and decision to submit the article for publication.

Declaration of Competing Interest

The authors declare that they have no known competing financial interests or personal relationships that could have appeared to influence the work reported in this paper.

Appendix A. Supplementary data

Supplementary data to this article can be found online at <https://doi.org/10.1016/j.radonc.2022.04.022>.

References

- [1] Jackson WC, Silva J, Hartman HE, Dess RT, Kishan AU, Beeler WH, et al. Stereotactic body radiotherapy for localized prostate cancer: a systematic review and meta-analysis of over 6,000 patients treated on prospective studies. *Int J Radiat Oncol* 2019;104:778–89. <https://doi.org/10.1016/j.ijrobp.2019.03.051>.
- [2] Widmark A, Gunnlaugsson A, Beckman L, Thellenberg-Karlsson C, Hoyer M, Lagerlund M, et al. Ultra-hypofractionated versus conventionally fractionated radiotherapy for prostate cancer: 5-year outcomes of the HYPO-RT-PC randomised, non-inferiority, phase 3 trial. *Lancet* 2019;394:385–95.
- [3] Brand DH, Tree AC, Ostler P, van der Voet H, Loblaw A, Chu W, et al. Intensity-modulated fractionated radiotherapy versus stereotactic body radiotherapy for prostate cancer (PACE-B): acute toxicity findings from an international, randomised, open-label, phase 3, non-inferiority trial. *Lancet Oncol* 2019;20:1531–43.
- [4] Dess RT, Jackson WC, Suy S, Soni PD, Lee JY, Abugharib AE, et al. Predictors of multidomain decline in health-related quality of life after stereotactic body radiation therapy (SBRT) for prostate cancer. *Cancer* 2017;123:1635–42.
- [5] King CR, Collins S, Fuller D, Wang P-C, Kupelian P, Steinberg M, et al. Health-related quality of life after stereotactic body radiation therapy for localized prostate cancer: results from a multi-institutional consortium of prospective trials. *Int J Radiat Oncol Biol Phys* 2013;87:939–45.
- [6] Bhattasali O, Chen LN, Woo J, Park J-W, Kim JS, Moures R, et al. Patient-reported outcomes following stereotactic body radiation therapy for clinically localized prostate cancer. *Radiat Oncol* 2014;9. <https://doi.org/10.1186/1748-717X-9-52>.
- [7] Boyer MJ, Papagikos MA, Kiteley R, Vujaskovic Z, Wu J, Lee WR. Toxicity and quality of life report of a phase II study of stereotactic body radiotherapy (SBRT) for low and intermediate risk prostate cancer. *Radiat Oncol* 2017;12:14. <https://doi.org/10.1186/s13014-016-0758-8>.
- [8] Lagendijk JJW, Raaymakers BW, van Vulpen M. The magnetic resonance imaging-linac system. *Semin Radiat Oncol* 2014;24:207–9. <https://doi.org/10.1016/j.semradonc.2014.02.009>.
- [9] Winkel D, Bol GH, Kroon PS, van Asselen B, Hackett SS, Werensteijn-Honingh AM, et al. Adaptive radiotherapy: The Elekta Unity MR-linac concept. *Clin Transl Radiat Oncol* 2019;18:54–9.
- [10] de Muinck Keizer DM, Kerkmeijer LGW, Willigenburg T, van Lier ALHMW, den Hartogh MD, van der Voort van Zyp JRN, et al. Prostate intrafraction motion during the preparation and delivery of MR-guided radiotherapy sessions. *Radiat Oncol* 2020;151:88–94. <https://doi.org/10.1016/j.radonc.2020.06.044>.
- [11] Muinck Keizer DM, Willigenburg T, der Voort van Zyp JRN, Raaymakers BW, Lagendijk JJW, Boer JCJ. Seminal vesicle intrafraction motion during the delivery of radiotherapy sessions on a 1.5 T MR-Linac. *Radiat Oncol J Eur Soc Ther Radiol Oncol* 2021;162:162–9.
- [12] Schaulé J, Chamberlain M, Wilke L, Baumgartl M, Krayenbühl J, Zamburlini M, et al. Intrafractional stability of MR-guided online adaptive SBRT for prostate cancer. *Radiat Oncol* 2021;16:189. <https://doi.org/10.1186/s13014-021-01916-0>.
- [13] Kontaxis C, de Muinck Keizer DM, Kerkmeijer LGW, Willigenburg T, den Hartogh MD, van der Voort van Zyp JRN, et al. Delivered dose quantification in prostate radiotherapy using online 3D cine imaging and treatment log files on a combined 1.5T magnetic resonance imaging and linear accelerator system. *Phys Imaging Radiat Oncol* 2020;15:23–9.
- [14] Menten MJ, Mohajer JK, Nilawar R, Bertholet J, Dunlop A, Pathmanathan AU, et al. Automatic reconstruction of the delivered dose of the day using MR-linac treatment log files and online MR imaging. *Radiat Oncol J Eur Soc Ther Radiol Oncol* 2020;145:88–94.
- [15] Hijab A, Tocco B, Hanson I, Meijer H, Nyborg CJ, Bertelsen AS, et al. MR-guided adaptive radiotherapy for bladder cancer. *Front Oncol* 2021;11. <https://doi.org/10.3389/fonc.2021.637591>.
- [16] Bohoudi O, Bruynzeel AME, Tetar S, Slotman BJ, Palacios MA, Lagerwaard FJ. Dose accumulation for personalized stereotactic MR-guided adaptive radiation therapy in prostate cancer. *Radiat Oncol* 2021;157:197–202. <https://doi.org/10.1016/j.radonc.2021.01.022>.
- [17] Wang K, Mavroidis P, Royce TJ, Falchook AD, Collins SP, Sapareto S, et al. Prostate stereotactic body radiation therapy: an overview of toxicity and dose response. *Int J Radiat Oncol Biol Phys* 2021;110:237–48.
- [18] Willigenburg T, de Muinck Keizer DM, Peters M, Claes An, Lagendijk JJW, de Boer HCJ, et al. Evaluation of daily online contour adaptation by radiation therapists for prostate cancer treatment on an MRI-guided linear accelerator. *Clin Transl Radiat Oncol* 2021;27:50–6.
- [19] de Muinck Keizer DM, van der Voort van Zyp JRN, de Groot-van Breugel EN, Raaymakers BW, Lagendijk JJW, de Boer HCJ. On-line daily plan optimization combined with a virtual couch shift procedure to address intrafraction motion in prostate magnetic resonance guided radiotherapy. *Phys Imaging Radiat Oncol* 2021;19:90–5.
- [20] Denis de Senneville B, Zachiu C, Ries M, Moonen C. EVolution: an edge-based variational method for non-rigid multi-modal image registration. *Phys Med Biol* 2016;61:7377–96. <https://doi.org/10.1088/0031-9155/61/20/7377>.
- [21] Bosma LS, Zachiu C, Ries M, Denis de Senneville B, Raaymakers BW. Quantitative investigation of dose accumulation errors from intra-fraction motion in MRgRT for prostate cancer. *Phys Med Biol* 2021;66:065002.
- [22] Zachiu C, Denis de Senneville B, Willigenburg T, Voort van Zyp JRN, de Boer JCJ, Raaymakers BW, et al. Anatomically-adaptive multi-modal image registration for image-guided external-beam radiotherapy. *Phys Med Biol* 2020;65:215028.
- [23] Willigenburg T, Zachiu C, Lagendijk JJW, van der Voort van Zyp JRN, de Boer HCJ, Raaymakers BW. Fast and accurate deformable contour propagation for intra-fraction adaptive magnetic resonance-guided prostate radiotherapy. *Phys Imaging Radiat Oncol* 2022;21:62–5.
- [24] Henderson DR, Murray JR, Gulliford SL, Tree AC, Harrington KJ, Van As NJ. An investigation of dosimetric correlates of acute toxicity in prostate stereotactic body radiotherapy: dose to urinary trigone is associated with acute urinary toxicity. *Clin Oncol (R Coll Radiol)* 2018;30:539–47. <https://doi.org/10.1016/j.clon.2018.05.001>.
- [25] Youden WJ. Index for rating diagnostic tests. *Cancer* 1950;3:32–5. [https://doi.org/10.1002/1097-0142\(1950\)3:1<32::AID-CNCR2820030106>3.0.CO;2-3](https://doi.org/10.1002/1097-0142(1950)3:1<32::AID-CNCR2820030106>3.0.CO;2-3).
- [26] Smith GA, Dunlop A, Barnes H, Herbert T, Lawes R, Mohajer J, et al. Bladder filling in patients undergoing prostate radiotherapy on a MR-linac: The dosimetric impact. *Tech Innov Patient Support Radiat Oncol* 2022;21:41–5.
- [27] de Muinck Keizer DM, Kerkmeijer LGW, Willigenburg T, van Lier ALHMW, Hartogh MDD, van der Voort van Zyp JRN, et al. Prostate intrafraction motion during the preparation and delivery of MR-guided radiotherapy sessions on a 1.5T MR-Linac. *Radiat Oncol* 2020;151:88–94.
- [28] Pathmanathan AU, van As NJ, Kerkmeijer LGW, Christodouleas J, Lawton CAF, Vesprini D, et al. Magnetic resonance imaging-guided adaptive radiation therapy: a “game changer” for prostate treatment? *Int J Radiat Oncol Biol Phys* 2018;100:361–73.
- [29] Alongi F, Rigo M, Figlia V, Cuccia F, Gaj-Levra N, Nicosia L, et al. 1.5 T MR-guided and daily adapted SBRT for prostate cancer: Feasibility, preliminary clinical tolerability, quality of life and patient-reported outcomes during treatment. *Radiat Oncol* 2020;15:1–9. <https://doi.org/10.1186/s13014-020-01510-w>.
- [30] Bruynzeel AME, Tetar SU, Oei SS, Senan S, Haasbeek CJA, Spoelstra FOB, et al. A prospective single-arm phase II study of stereotactic magnetic-resonance-guided adaptive radiotherapy for prostate cancer: Early toxicity results. *Int J Radiat Oncol* 2019. <https://doi.org/10.1016/j.ijrobp.2019.08.007>.
- [31] Li S, Boyer A, Lu Y, Chen GT. Analysis of the dose-surface histogram and dose-wall histogram for the rectum and bladder. *Med Phys* 1997;24:1107–16. <https://doi.org/10.1118/1.598014>.
- [32] Maggio A, Carillo V, Cozzarini C, Perna L, Rancati T, Valdagni R, et al. Impact of the radiotherapy technique on the correlation between dose-volume histograms of the bladder wall defined on MRI imaging and dose-volume/surface histograms in prostate cancer patients. *Phys Med Biol* 2013;58:N115–23. <https://doi.org/10.1088/0031-9155/58/7/n115>.